On the Improved Method for the Mode Shapes of a Curved Beam in a Drum Brake

Byoung Duk Lim*, Kyu Kang Jung*, Ki Hyun Yoon*, Du Shik Shin**

ABSTRACT

The squeal vibration of a drum brake is the major source of brake noise. In this study the binary flutter model of squeal vibration was employed for the drum brake of a passenger car. The vibration analysis of a drum brake was performed by using normal modes, which are obtained by variational method. An improved method for the estimation of shoe modes is proposed and the results are compared with the exact solutions. Numerical results for the coupled system of drum and shoes show good agreement with the results of experimental modal analysis and those obtained by FE analysis.

I. Introduction

Squeal vibration and noise of the automobile brake system have attracted much attention as the other parts become quieter. In case of the drum brake, friction induced vibration of coupled system, so called binary flutter, is considered to be the most prominent mechanism underlying squeal phenomena instead of the classical stick-slip model.

Stick-slip vibration occurs when the friction coefficient μ is dependent on the relative velocity of the lining material with respect to the drum, especially when μ-v curve has negative slope. If the damping of the system is less than the slope of μ-v curve multiplied by the normal force, which is usually exerted by hydraulic or pneumatic actuators, total damping effort given to the system becomes negative, i.e., vibration energy is pumped in rather than being removed.

While stick-slip occurs when the friction coefficient μ depends on the relative velocity, especially when μ-v curve has negative slope, binary flutter occurs even when μ is constant over some velocity range. In this model the lining material is considered as a soft elastic material while the drum and backplate of the shoe are considered to be rigid. Therefore the lining thickness is determined by the relative displacement between drum and backplate, and in turn the pressure, proportional to the thickness variation, also depends on the radial displacements of both structures. This change in the radial force results in the friction force variation. If the drum and shoes are modeled as a thin shell or its section, the dominant mode of vibration is the flexural vibration and the circumference of the neutral surface of each structure remains unchanged. Therefore coupling of the radial and circumferential displacement due to zero hoop strain and coupling of the normal and friction force result in a positive feedback and cause the unstable responses generating high intensity sound.

This model was first proposed by North [1] considering brake system as a lumped parameter system. Millner [2] considered the drum brake as a cylindrical shell and the shoes as curved beams. Okamura and Nishiwaki [3] developed an improved analytical model and studied the effect of friction coefficient on the stability. Lang et al. [4] developed an experimental modal analysis technique for rotational modes and showed that the noise generation is mainly due to binary flutter. They also have investigated the complex modes resulting in the squeal vibration. Day and Kim [5] used FEM for modal analyses of S-cam drum brake.

In Okamura and Nishiwaki's model the coupling effect of drum vibration with the shoe through friction material requires the information about the mode shapes of the curved bar. In this study an improved eigenvalue approximation is proposed for the curved beam, which is essential in estimating the coupled system's mode shapes. The calculated characteristic values showed good agreement with the exact solutions. Experimental verifications are also given to support the usefulness of the proposed method.

* Department of Mechanical Engineering Yeungnam University
** Sangshin Brake Co.

Manuscript Received May 8, 1996.

I. Vibration of a cylindrical shell under the action of the friction forces and pressure

Although a brake drum is an open cylindrical shell of finite length with an end cap, it can be assumed to be one with both ends open. This assumption is based on the experimental results of modal analysis especially at the lower order modes. Also shoes are considered as sections of cylindrical shell with uniform cross section or curved free-free beams. Figure 1

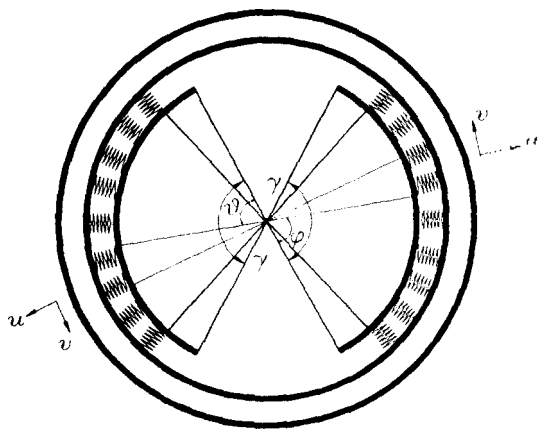

Fig 1. Geometry of drum brake system

shows simplified geometrical configuration of the brake system. Here a shoe is named as the leading shoe and the other as the trailing shoe. Since the lining material between the drum and shoes has smaller elastic modulus (usually much less than 1/10 of steel) compared to the structure material, its thickness is assumed to be determined by the relative radial displacement between the drum and shoes. Therefore the pressure on the drum exerted by the lining material can be represented as the product of Young's modulus and the normal strain of the lining material.

$$R_{sp}=\frac{E_l}{h}\,(u_{sp}-u_d)\,d\phi$$

$$R_{ss}=\frac{E_l}{h}\,(u_{ss}-u_d)\,d\theta$$

where u's are the radial displacements, the subscripts d, sp and ss denote the drum, leading shoe and trailing shoe respectively, E_l is the Young's modulus, and h is the thickness of the lining material.

If the friction coefficient μ is considered to be constant regardless of the relative speed, then the shear stress on the contact surface is proportional to the normal pressure as

$$F_{sp}=\mu R_{sp}$$

$$F_{ss}=\mu R_{ss}$$

Since the forces considered are in radial and circumferential directions, the axial force may be neglected and only the radial and circumferential displacements are to be taken into account. Moreover since the thickness of the drum is much less than the radius, the drum and shoes are modeled as thin cylindrical shell or its section where the only considerable mode of vibration is the flexural vibration. From the characteristics of the small deflection of bending vibration it can be assumed that the circumference of the neutral surface of each structures remains unchanged, which means the hoop strain of a cylindrical shell is zero, i.e.

$$(\varepsilon_\phi)_d=\frac{u_d}{r}+\frac{1}{r}\frac{\partial v_d}{\partial\phi}=0$$

where u_d and v_d represent the radial and circumferential displacements. Therefore due to the zero hoop strain condition the radial displacement is coupled with the circumferential displacement such that

$$u_d=-\frac{\partial v_d}{\partial\phi} \tag{1}$$

The radial and circumferential displacements of drum need to be functions of ϕ with periodicity of 2π as follows;

$$u_d=A_1\cos\phi+A_2\cos 2\phi+\cdots+B_1\sin\phi+B_2\sin 2\phi+\cdots \tag{2}$$

$$v_d=-A_1\sin\phi-\frac{A_2}{2}\sin 2\phi-\cdots+B_1\cos\phi-\frac{B_2}{2}\cos 2\phi+\cdots$$

The sth modal displacements can be represented as

$$\begin{bmatrix}u_{ds}\\ v_{ds}\end{bmatrix}=\begin{bmatrix}-\frac{\partial\Phi_{1s}}{\partial\phi} & -\frac{\partial\Phi_{2s}}{\partial\phi}\\ \Phi_{1s} & \Phi_{2s}\end{bmatrix}\begin{bmatrix}q_{1s}(t)\\ q_{2s}(t)\end{bmatrix} \tag{3}$$

where $\Phi_{1s}=-\sin s\phi/s$, $\Phi_{2s}=\cos s\phi/s$, (s:integer) and $q_{1s}(t)$ and $q_{2s}(t)$ are generalized coordinates of the s-th mode. Deformation energy of the drum [6], U_d, is

$$U_d=\int_{volume}\frac{\sigma^2}{2E_d}\,dV=\frac{1}{2E_d}\int\frac{M^2 l_d}{I_z}\,d\phi$$

$$=E_d\frac{I_z}{2l_d^4}\int_0^{2\pi}\left(\frac{\partial^2 u_d}{\partial\phi^2}+u_d\right)^2 d\phi$$

where E_d and l_d are the Young's modulus and radius of the drum and I_z is the area moment of inertia. The overall kinetic energy, T_d, is

$$T_d=\frac{l_d\rho A_d}{2}\int_0^{2\pi}(\dot{u}_d^2+\dot{v}_d^2)^2\,d\varphi$$

Substituting the expressions of u_d and using the orthogonality of trigonometric functions kinetic and strain energies can be represented in terms of the generalized coordinates $q_{1s}(t)$ and $q_{2s}(t)$ as

$$T_d=\frac{l_d\rho_d A_d\pi}{2}\sum_{s=1}^{\infty}(1+\frac{1}{s^2})(\dot{q}_{1s}^2+\dot{q}_{2s}^2) \tag{4}$$

$$U_d=\frac{E_d I_z\pi}{2l_d^3}\sum_{s=1}^{\infty}(1-s^2)^2(q_{1s}^2+q_{2s}^2) \tag{5}$$

Similarly the deformation and kinetic energies of shoe are

$$T_{sp}=\frac{l\rho A}{2}\int_{\gamma_1}^{\gamma_2}(u_{sp}^2+v_{sp}^2)^2\,d\varphi$$

$$U_{sp}=\frac{EI}{2l^4}\int_{\gamma_1}^{\gamma_2}(\frac{\partial^2 u_{sp}}{\partial\varphi^2}+u_{sp})^2\,d\varphi$$

for the leading shoe, while those of trailing shoe can be obtained by replacing the integration interval with $[\beta_1, \beta_2]$ as

$$T_{ss}=\frac{l\rho A}{2}\int_{\beta_1}^{\beta_2}(u_{ss}^2+v_{ss}^2)^2\,d\theta$$

$$U_{ss}=\frac{EI}{2l^4}\int_{\beta_1}^{\beta_2}(\frac{\partial^2 u_{ss}}{\partial\theta^2}+u_{ss})^2\,d\theta$$

Also the displacements are represented in terms of generalized coordinates as follows.

$$\begin{bmatrix}u_{sp}\\v_{sp}\end{bmatrix}=\begin{bmatrix}-\frac{\partial\Phi_p}{\partial\phi}\\\Phi_p\end{bmatrix}[q_{sp}(t)] \tag{6}$$

$$\begin{bmatrix}u_{ss}\\v_{ss}\end{bmatrix}=\begin{bmatrix}-\frac{\partial\Phi_s}{\partial\theta}\\\Phi_s\end{bmatrix}[q_{ss}(t)] \tag{7}$$

where $\Phi_p(\phi)$ and $\Phi_s(\phi)$ are the mode shape functions derived in the following section.

The generalized force corresponding to the ith generalized coordinate Q_{di} on the drum can be expressed as

$$Q_{di}=\int_{\gamma_1}^{\gamma_2}(\frac{\partial R_{sp}}{\partial\varphi}\frac{\partial u_d}{\partial q_{di}}+\frac{\partial F_{sp}}{\partial\varphi}\frac{\partial v_d}{\partial q_{di}})\,d\varphi+$$
$$+\int_{\beta_1}^{\beta_2}(\frac{\partial R_{ss}}{\partial\theta}\frac{\partial u_d}{\partial q_{di}}+\frac{\partial F_{ss}}{\partial\theta}\frac{\partial v_d}{\partial q_{di}})\,d\theta. \tag{8}$$

Also the generalized force on the shoes are

$$Q_{sp}=\int_{\gamma_1}^{\gamma_2}(-\frac{\partial R_{sp}}{\partial\phi}\frac{\partial u_{sp}}{\partial q_{sp}}-\frac{\partial F_{sp}}{\partial\phi}\frac{\partial v_{sp}}{\partial q_{sp}})\,d\phi \tag{9}$$

$$Q_{ss}=\int_{\beta_1}^{\beta_2}(-\frac{\partial R_{ss}}{\partial\theta}\frac{\partial u_{ss}}{\partial q_{ss}}-\frac{\partial F_{ss}}{\partial\theta}\frac{\partial v_{ss}}{\partial q_{ss}})\,d\theta \tag{10}$$

for the leading and trailing shoes respectively.

Applying Euler-Lagrange equation, the equations of motion of the coupled system for the s-th mode is derived as follows.

$$M\ddot{X}+KX=LAX+\mu LBX \tag{11}$$

where

$$M=\begin{bmatrix}m_{ss}&0&\\&m_{sp}&\\&&m_{d1}\\0&&&m_{d2}\end{bmatrix}\quad M=\begin{bmatrix}K_{ss}&0&\\&K_{sp}&\\&&K_{d1}\\0&&&K_{d2}\end{bmatrix}$$

$$A=\begin{bmatrix}a_{11}&0&a_{13}&a_{14}\\&a_{22}&a_{23}&a_{24}\\SYM&&a_{33}&a_{34}\\&&&a_{44}\end{bmatrix}\quad B=\begin{bmatrix}b_{11}&0&b_{13}&b_{14}\\0&b_{22}&b_{23}&b_{24}\\b_{31}&b_{32}&b_{33}&b_{34}\\b_{41}&b_{42}&b_{43}&b_{44}\end{bmatrix}$$

$$X=\begin{bmatrix}q_{ss}(t)\\q_{sp}(t)\\q_{d1}(t)\\q_{d2}(t)\end{bmatrix}$$

The detailed expressions of the coefficient matrices are given in the appendix.

Ⅲ. Derivation of the mode shape functions.

In calculating the elements of the matrices in Eq. (11) the mode shape functions of circularly curve beam is required (see the appendix). The equation of motion of the circularly curved beam is

$$\frac{1}{K^2}\cdot\ddot{u}+(1+\frac{\partial^2}{\partial\phi^2})(u+\frac{\partial^2 u}{\partial\phi^2})=0 \tag{12}$$

where $\frac{1}{K}=\sqrt{\frac{l^3\rho\sigma}{EI}}$

Using separation of variables and assuming harmonic motion, u can be written as

$$u(\phi,t)=\Phi(\phi)\cdot f(t)=\Phi(\phi)(A\cos\omega t+B\sin\omega t)$$

above equation becomes an ordinary differential equation with constant coefficients as

$$\frac{\partial^4\Phi}{\partial\phi^4}+2\frac{\partial^2\Phi}{\partial\phi^2}+(1-\frac{\omega^2}{K^2})\Phi=0 \tag{13}$$

whose solution has the form of $\Phi(\phi)=e^{\lambda\phi}$. Then the differential equation becomes a characteristic equation as

$$\lambda^4+2\lambda^2+(1-\frac{\omega^2}{K^2})=0 \tag{14}$$

where $\frac{\omega^2}{K^2} = \alpha^4$ ($\alpha^4 \gg 1$). General solution of $\Phi(\phi)$ for the leading shoe, Φ_p is given as

$$\Phi_p(\phi) = A\cos\lambda_1(\phi - \frac{\gamma}{2}) + B\sin\lambda_1(\phi - \frac{\gamma}{2})$$
$$+ C\cosh\lambda_3(\phi - \frac{\gamma}{2}) + D\sinh\lambda_3(\phi - \frac{\gamma}{2})$$

If the solutions are grouped as a symmetric part including cosine and cosh functions and an anti-symmetric part with remaining terms, from the boundary conditions of a free-free beam the characteristic values of each part can be calculated by the characteristic equations given as

$$\begin{bmatrix} (\lambda_1^2 - 1)\cos\frac{\lambda_1\gamma}{2} & -(\lambda_3^2 + 1)\cosh\frac{\lambda_3\gamma}{2} \\ (\lambda_1^3 - 1)\sin\lambda_1\gamma & (\lambda_3^3 + \lambda_3)\sinh\lambda_3\gamma \end{bmatrix} \begin{bmatrix} A \\ C \end{bmatrix} = \begin{bmatrix} 0 \\ 0 \end{bmatrix}$$

for symmetric parts and

$$\begin{bmatrix} -(\lambda_1^2 - 1)\sin\frac{\lambda_1\gamma}{2} & (\lambda_3^2 + 1)\sinh\frac{\lambda_3\gamma}{2} \\ -(\lambda_1^3 - \lambda_1)\cos\lambda_1\gamma & (\lambda_3^3 + \lambda_3)\cosh\lambda_3\gamma \end{bmatrix} \begin{bmatrix} B \\ D \end{bmatrix} = \begin{bmatrix} 0 \\ 0 \end{bmatrix}$$

for antisymmetric part. This yields two independent equations with respect to λ_1 and λ_3 as

$$\frac{\lambda_1\gamma}{2}\tan\frac{\lambda_1\gamma}{2} = -\frac{\lambda_3\gamma}{2}\tanh\frac{\lambda_3\gamma}{2} \quad \text{for symmetric part} \quad (15)$$

and $\frac{\lambda_1\gamma}{2}\cot\frac{\lambda_1\gamma}{2} = -\frac{\lambda_3\gamma}{2}\coth\frac{\lambda_3\gamma}{2}$ for antisymmetric part (16)

where $\lambda_1^2 = \alpha^2 + 1$ and $\lambda_3^2 = \alpha^2 - 1$

Although these equations can be solved numerically, a closed form approximation can make it easy to determine the matrix elements in closed forms. For $\alpha \gg 1$, λ_1 and λ_3 can be approximated as

$$\lambda_1 \simeq \alpha(1 + \frac{1}{2\alpha^2}) \simeq \frac{1}{2\alpha} \quad (17)$$
$$\lambda_3 = \alpha(1 + \frac{1}{2\alpha^2}) \simeq \alpha - \frac{1}{2\alpha}.$$

For large α the Eq. (15) is approximately $\tan(\lambda_1\gamma/2) = -\tanh(\lambda_3\gamma/2)$. Denoting m as the solution of this equation, α can be expressed as $\frac{\alpha\gamma}{2} = \frac{m}{2} + x$ where x is the perturbation variable. Substituting this into the Eq. (15) and denoting m_n as the nth solution of $\tanh m = -\tan m$, and letting $x_n = x + \frac{\gamma^2}{4m_n}$, the right hand side of the characteristic equation is rearranged using these variables as

$$(m_n + x_n)\tan(m_n + x_n) = (m_n + x_n)\frac{\tan m_n + \tan x_n}{1 - \tan m_n \cdot \tan x_n}$$

Since m_n is very near to $(4n-1)\pi/4$, $(n = 1, 2, \cdots)$ the above equation can be simplified as $(m_n + x_n)\frac{-1 + \tan x_n}{1 + \tan x_n}$
$= -(m_n + x_n)\frac{-1 + \tan x_n}{1 + \tan x_n}$

Using the smallness of x_n and y_n, the left hand side becomes $(m_n + y_n)\tanh(m_n + y_n) \simeq (m_n + y_n)$ and the right hand side becomes $(m_n + x_n)(1 - 2x_n) = (m_n + y_n)$.

From this equation the expression of x is given as follows.

$$x = -\frac{\gamma^2}{2} m_n^2\left(\frac{m_n}{2} - 1\right) \quad (18)$$

Therefore the symmetric mode shape function is given as

$$\Phi_p = \cosh\lambda_3(\phi - \frac{\gamma}{2}) + \frac{\lambda_3^2 + 1}{\lambda_1^2 - 1}\cdot\frac{\cosh\frac{\lambda_3\gamma}{2}}{\cos\frac{\lambda_1\gamma}{2}}\cdot\cos\lambda_1(\phi - \frac{\gamma}{2}). \quad (19)$$

$$\lambda_1 = \frac{2}{\gamma}\left(m_n + x + \frac{\gamma^2}{4m_n}\right),\ \lambda_3 = \frac{2}{\gamma}\left(m_n + x + \frac{\gamma^2}{4m_n}\right) \quad (20)$$

The Eq. (16) gives the same solutions as Eq. (20) except that m_n in this case is $\frac{(4n+1)\pi}{4}$. Similarly the shape functions for anti-symmetric mode can be obtained as

$$\Psi_p = \sinh\lambda_3(\phi - \frac{\gamma}{2}) + \frac{\lambda_3^2 + 1}{\lambda_1^2 - 1}\cdot\frac{\sinh\frac{\lambda_3\gamma}{2}}{\sin\frac{\lambda_1\gamma}{2}}\cdot\sin\lambda_1(\phi - \frac{\gamma}{2}). \quad (19)$$

Ⅳ. Numerical results and discussions

Before proceeding further the approximate solution of the characteristic equation for a curved beam proposed in this study is compared with those given by Okamura et al. [3]. Table Ⅰ shows the results, where the exact values are obtained through numerical analysis of the Eq. (15). As is seen in the Table Ⅰ, the improved method gives much better results especially in the lower modes which is of more significance in squeal vibration analysis.

Once the mode shape functions are determined, Eq. (11) becomes another characteristic equation with respect to the frequency ω where the eigenvectors correspond to the mode shapes in terms of generalized coordinates. Table Ⅱ shows modal frequencies calculated by the present method and those measured by impact tests.

The first two frequencies coincide with the measured ones though the 3rd and 4th components show discrep-

Table 1. Solutions of eq.(7) by various methods

	numerical analysis of Eq.(15)		improved method		Okamura et al. [3]	
order	λ_1	λ_3	λ_1	λ_3	λ_1	λ_3
1	2.18	1.66	2.15	1.66	1.89	1.16
2	4.79	4.58	4.79	4.58	4.74	4.43
3	7.51	7.37	7.51	7.37	7.49	7.29
4	10.23	10.13	10.23	10.13	10.22	10.07
5	12.96	12.88	12.96	12.88	12.95	12.85

Table 2. Modal frequencies calculated by the improved method, and FEM, and from measurement.

[unit : Hz]

Order / Method	1	2	3	4
Calculation	938.83	2645.75	3088.47	5070.56
Measurement	945.35	2648.80	3244.0	4394.5
F E M	1001.7	2783.0	3438.2	4756.0

ancy of about 5% and 15%. Also frequencies predicted by finite element method shows similar but a little higher than those measured. However, this result looks quite satisfactory because dominant squeal frequencies lie in the range between 1 and 6 kHz. Figures 2-5 show the mode shapes corresponding to each modal frequency. For a modal

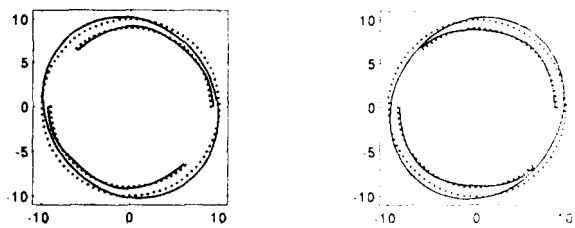

Fig 4. Calculated mode shape pair at f = 3088Hz

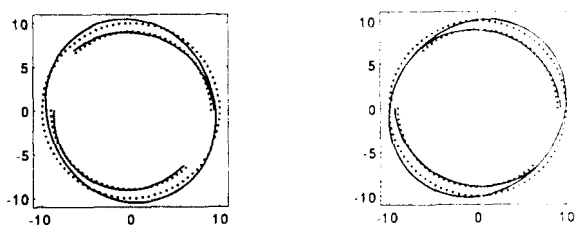

Fig 2. Calculated mode shape pair at f = 938Hz

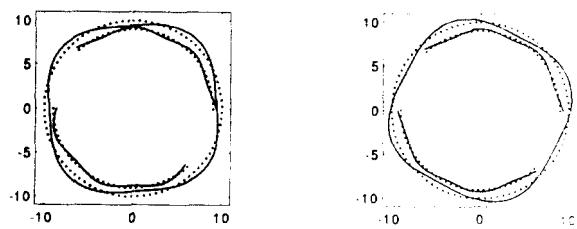

Fig 5. Calculated mode shape pair at f = 5070Hz

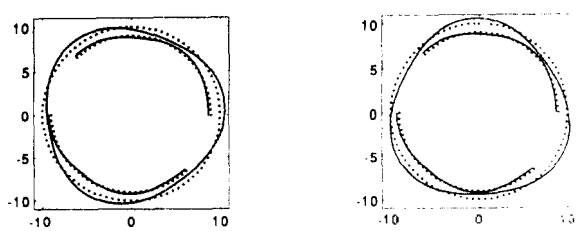

Fig 3. Calculated mode shape pair at f = 2646Hz

frequency a pair of mode shapes are possible as shown in these figures. Actually these are a complex conjugate pair. This kind of degeneracy is usually called doublet modes and has no preferred angular positions [5]. Fig. 6 shows 4 mode shapes of drum measured by impact test. Mode shapes look similar to those calculated respectively.

While the drum is modelled as an open cylinder of finite length and deformation of the hub is neglected in this study, the hub motion becomes significant at higher

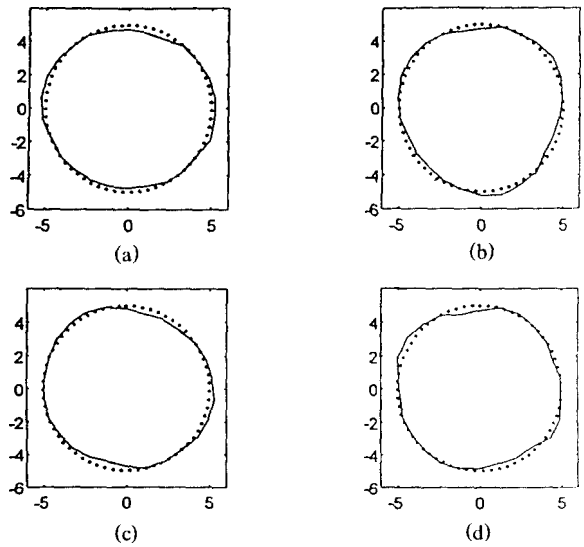

Fig 6. Measured mode shapes at
(a) 945 Hz (b) 2649 Hz (c) 3244 Hz (d) 4394 Hz

order modes and a more elaborate model is required to take this into account. This may be the major reason of the discrepancy in the 4th order modal frequency from those maesured and FE anlysis as shown in the Table II.

Conclusions

Using an analytical dynamic model and normal mode functions, a system of equations of motion of the drum brake is derived. In order to get a closed form expression for the coefficient matrix an improved method to obtain the characteristic values is proposed for the vibration analysis of a curved beam. Comparing with the numerical analysis results it is found that the present method gives better results than those given by Okamura et al. [3]. Furthermore the calculated natural frequencies showed good agreement with measured ones at the 1st and 2nd modes but some discrepancy of about 5 and 15% at the 3rd and 4th modes. Calculated mode shapes look almost same as those measured up to 4th mode.

Acknowledgement

This work has been supported by Sangshin Brake Co. and the Yeungnam Regional Consortium.

References

1. M. R. North, "Disc brake squeal-a theoretical model," Proc. of the IMechE Conf. on Braking of road vehicles, C38/76, pp. 169-176, 1976.
2. N. A. Millner, "A theory of drum brake squeal," Proc. of the IMechE Conf. on Braking of road vehicles, C39/76, pp. 177-185, 1976.
3. H. Okamura and M. Nishiwaki, "A study on brake noise (drum brake squeal)," JSME International J., vol. 32, pp. 206-214, 1989.
4. A. M. Lang, T. P. Newcomb, and P. C. Brooks, "Brake squeal-the influence of rotor geometry," Proc. of the IMechE Conf. on Braking of road vehicles, C444/016/93, pp. 161-171, 1993.
5. A. J. Day and S. Y. Kim, "Noise and vibration analysis of an S-cam drum brake," Proc. IMechE, Part D, vol. 210, pp. 35-43, 1996.
6. W. Weaver,Jr., S. P. Timoshenko and D. H. Young, *Vibration Problems in Engineering*, Wiley, 1990

Appendix.

Elements of the Coefficient Matrix in Eq.(11)

$$M\ddot{X}+KX=LAX+\mu LBX$$

$$M=\begin{vmatrix} m_{ss} & & 0 & \\ & m_{sp} & & \\ & & m_{d1} & \\ 0 & & & m_{d2} \end{vmatrix} \qquad K=\begin{vmatrix} K_{ss} & & 0 & \\ & K_{sp} & & \\ & & K_{d1} & \\ 0 & & & K_{d2} \end{vmatrix}$$

$$A=\begin{vmatrix} a_{11} & 0 & a_{13} & a_{14} \\ & a_{22} & a_{23} & a_{24} \\ SYM & & a_{33} & a_{34} \\ & & & a_{44} \end{vmatrix} \qquad B=\begin{vmatrix} b_{11} & 0 & b_{13} & b_{14} \\ 0 & b_{22} & b_{23} & b_{24} \\ b_{31} & b_{32} & b_{33} & b_{34} \\ b_{41} & b_{42} & b_{43} & a_{44} \end{vmatrix}$$

$$X=\begin{vmatrix} q_{ss}(t) \\ q_{sp}(t) \\ q_{d1}(t) \\ q_{d2}(t) \end{vmatrix}$$

$$m_{ss} = l\rho\sigma\int_0^{\gamma}\left\{\left(-\frac{d\psi_s}{d\theta}\right)^2+\psi_s^2\right\}d\theta \quad , \quad m_{sp} = \rho\sigma\int_0^{\gamma}\left\{\left(-\frac{d\psi_p}{d\phi}\right)^2+\psi_p^2\right\}d\phi \quad , \quad m_{d1} = m_{d2} = \pi I_d\rho_d\sigma_d\left(1+\frac{1}{S^2}\right)$$

$$K_{ss} = \frac{EI}{l^3}\int_0^{\gamma}\left\{\left(\frac{d\psi_s}{d\theta}+\frac{d^3\psi_s}{d\theta^3}\right)^2\right\}d\theta \quad , \quad K_{sp} = \frac{EI}{l^3}\int_0^{\gamma}\left\{\left(-\frac{d\psi_{sp}}{d\phi}+\frac{d^3\psi_{sp}}{d\phi^3}\right)^2\right\}d\phi \quad , \quad K_{d1} = K_{d2} = \frac{\pi E_d I_d}{l_d^3}(S^2-1)^2$$

$$a_{11} = -\int_{\beta_1}^{\beta_2}\left(\frac{d\psi_s}{d\theta}\right)^2 d\theta \quad , \quad a_{22} = -\int_{\gamma_1}^{\gamma_2}\left(\frac{d\psi_p}{d\phi}\right)^2 d\phi \quad , \quad a_{13} = -\int_{\beta_1}^{\beta_2}\sin S(\theta+\alpha)\frac{d\psi_s}{d\theta}\,d\theta$$

$$a_{14} = \int_{\beta_1}^{\beta_2}\cos S(\theta+\alpha)\frac{d\psi_s}{d\theta}\,d\theta \quad , \quad a_{23} = -\int_{\gamma_1}^{\gamma_2}\sin S\phi\frac{d\psi_p}{d\phi}\,d\phi \quad , \quad a_{24} = \int_{\gamma_1}^{\gamma_2}\cos S\phi\frac{d\psi_p}{d\phi}\,d\phi$$

$$a_{33} = -\int_{\gamma_1}^{\gamma_2}\sin^2 S\phi d\phi - \int_{\beta_1}^{\beta_2}\sin^2 S(\theta+\alpha)d\theta \quad , \quad a_{34} = \int_{\gamma_1}^{\gamma_2}\sin S\phi\cos S\phi d\phi + \int_{\beta_1}^{\beta_2}\sin S(\theta+\alpha)\cos S(\theta+\alpha)d\theta$$

$$a_{44} = -\int_{\gamma_1}^{\gamma_2}\cos^2 S\phi d\theta - \int_{\beta_1}^{\beta_2}\cos^2 S(\theta+\alpha)\,d\theta \quad , \quad b_{11} = \int_{\beta_1}^{\beta_2}\psi_s\frac{d\psi_s}{d\theta}\,d\theta \quad , \quad b_{22} = \int_{\gamma_1}^{\gamma_2}\psi_p\frac{d\psi_p}{d\phi}\,d\phi$$

$$b_{13} = \int_{\beta_1}^{\beta_2}\sin S(\theta+\alpha)\psi_s d\theta \quad , \quad b_{14} = -\int_{\beta_1}^{\beta_2}\cos S(\theta+\alpha)\psi_s d\theta \quad , \quad b_{23} = \int_{\gamma_1}^{\gamma_2}\sin S\phi\psi_p d\phi$$

$$b_{24} = -\int_{\gamma_1}^{\gamma_2}\cos S\phi\psi_p d\phi \quad , \quad b_{33} = -\frac{1}{S}\int_{\gamma_1}^{\gamma_2}\sin S\phi\cos S\phi d\phi - \frac{1}{S}\int_{\beta_1}^{\beta_2}\sin S(\theta+\alpha)\cos S(\theta+\alpha)d\theta$$

$$b_{44} = \frac{1}{S}\int_{\gamma_1}^{\gamma_2}\sin S\phi\cos S\phi d\phi + \frac{1}{S}\int_{\beta_1}^{\beta_2}\sin S(\theta+\alpha)\cos S(\theta+\alpha)d\theta \quad , \quad b_{31} = -\frac{a_{14}}{S}$$

$$b_{32} = -\frac{a_{24}}{S} \quad , \quad b_{34} = -\frac{a_{44}}{S} \quad , \quad b_{41} = \frac{a_{13}}{S} \quad , \quad b_{42} = \frac{a_{23}}{S} \quad , \quad b_{43} = \frac{a_{33}}{S}$$

▲Byoung-Duk Lim

1977: BS in Mechanical Engineering, Seoul National University

1979: MS in Mechanical Engineering, KAIST

1987: Ph.D. in Mechanical Engineering, KAIST

1985~1993: Research Scientist at Korea Research Institute of Standards and Science

1993~present: Assistant Professor in the Dept. of Mechanical Engineering, Yeungnam University.

▲Kyun Kang Jung

1993: BS in Mechanical Engineering, Yeungnam University.

1993~1994: Engineer, Pacific Chemical Co.

1996: MS in Mechanical Engineering, Yeungnam University.

1996~present: Researcher, R&D Center, Samsung Aerospace Ind.

▲Ki Hyun Yoon

1994: BS in Mechanical Engineering, Yeungnam University.

1996: MS in Mechanical Engineering, Yeungnam University.

1996~present: Researcher, R&D center, Mando Machincry Corp.

▲Doo-Shik Shin

1981: BS in Material Engineering, Hanyang University

1983: MS in Material Engineering, Hanyang University

1993: Ph.D in Material Science, Stevens Institute of Technology

1993~present: General Manager of the R&D dept., Sangshin Brake Ind.